Contents

Chapter 1

Cyclotron

In addition to the cyclotron accelerator, this first chapter introduces preliminary beam optics notions, including orbit, field index, periodic stability, optical functions, together with a key optical element: the dipole magnet. These concepts will be manipulated throughout the course. The chapter also familiarizes with raytracing and computer program simulations, starting with short, simple, optical sequences.

1.1   Introduction

The cyclotron arrived at a time, $\sim$1930 [1] (Fig. 1.1), where techniques to accelerate ions were sought, for the study of nuclear properties of the atom. To this day, hundreds of cyclotrons have been built, and more still are, to accelerate protons, ions, radioactive isotopes. They find application in "particle factories" (production of high flux beams of muons, neutrons, etc., Fig. 1.2), protontherapy (Fig. 1.3), production of radio-isotopes for medicine, and more. Cryogeny technologies allow further progress towards compactness (Fig. 1.3), and towards higher rigidities [2] (Fig. 1.4).
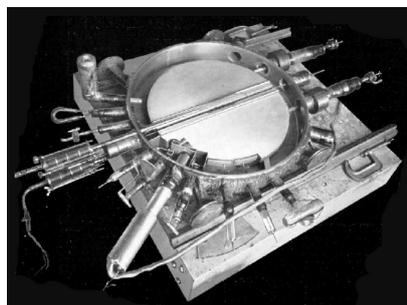

Fig. 1.1   An early cyclotron, late 1930s.
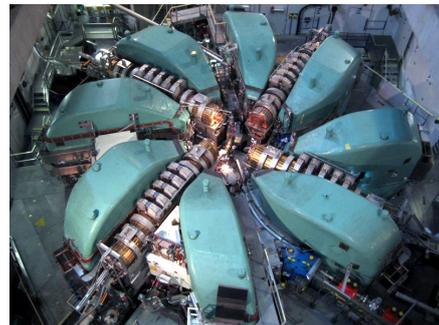
Fig. 1.2   The high power CW proton cyclotron at PSI, 1.4 MW today steadily increasing with years. It delivers a 590 MeV beam for secondary particle production (*e.g.*, neutron, muon).

The cyclotron combined together two long known concepts: resonant acceler-

2   *Cyclotron*


Fig. 1.3   Superconducting-coil isochronous spiral-sector AVF cyclotron at PSI, providing 250 MeV, 500 nA beams for hadrontherapy.
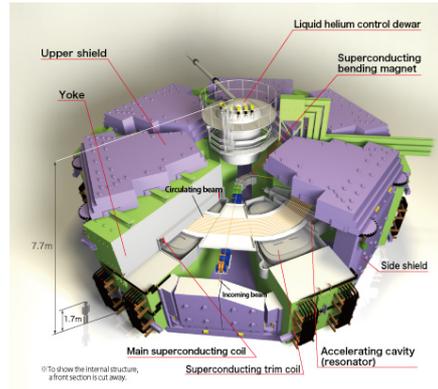

Fig. 1.4   RIKEN superconducting-coils separated-sector K*** heavy ion cyclotron, a compact, $\sim$ 20 m diameter, K-***, *** GeV proton equivalent rigidity [2].

ation through electric gaps, and trajectory bending by a magnetic field. It was conceived as a means to overcome the inconvenient of using a long series of high voltage electrodes in a linear layout, by, instead, repeated recirculation using a magnetic field, for incremental, resonant, energy gain through a single accelerating gap. This gap is formed by a pair of cylindrical electrodes, the "dees" (Figs. 1.5). which are applied a fixed frequency oscillating voltage, generated using a radio transmitter. The dees are plunged in a uniform magnetic field which causes the ion bunches to follow, as they are accelerated, a piecewise-circular path with increasing radius, normal to the field, in synchronism with the voltage oscillation. Here lies
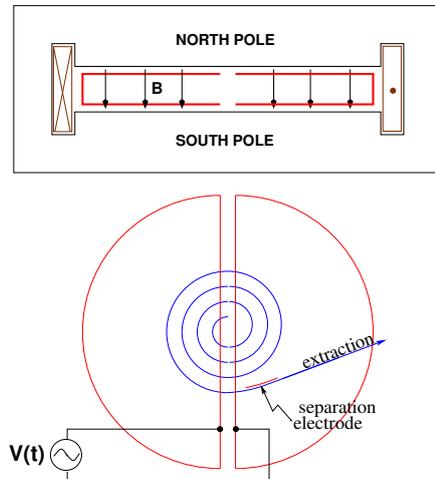
Fig. 1.5   Cyclotron : trajectories spiral in the uniform magnetic field between two circular poles. A double-dee forms a gap which is applied an oscillating voltage V(t) with frequency an integer multiple h of the revolution frequency, causing particles with the proper phase with respect to V(t) to be accelerated at each crossing. Bunch extraction is obtained by way of a separation electrode, located in the region etween the last two turns. *In passing: check the consistency of the coil current, direction of $\vec{B}$ and particle rotation - what is the sign of the accelerated particles?*
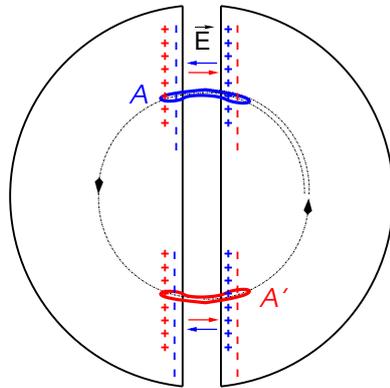
Fig. 1.6   Resonant acceleration: a bunch meeting an accelerating field $\vec{E}$ across the gap at A, at time t, will meet again, half a revolution later, at time $t + T_{\mathrm{rev}}/2 = t + hT_{\mathrm{rf}}/2$, an accelerating field $\vec{E}$ across the gap at A', and so forth turn after turn.

the cyclotron idea: while an accelerated bunch spirals outward, the increase in the distance it travels over a turn is compensated by its velocity increase: in the non-relativistic approximation ($\gamma \approx 1$), the revolution time T_{rev} remains quasi-constant; with the appropriate voltage frequency $f_{\mathrm{rf}} \approx h/T_{\mathrm{rev}}$ revolution motion and RF can be maintained in close synchronism, $T_{\mathrm{rev}} \approx hT_{\mathrm{rf}}$, so that the bunch transit the accelerating gaps during the accelerating phase of V(t) (Fig. 1.6).

A common method for a realistic modeling of the magnetic field of a cyclotron dipole magnet is to use a field map. Using a mathematical model is also a reasonable approach in a preliminary design phase, in particular it brings flexibility to tweak parameters such as field homogeneity, radial or azimuthal field dependence. These two techniques are employed in the exercises to come.
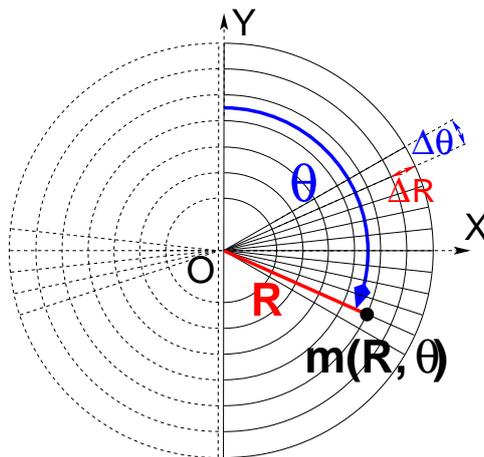
Fig. 1.7   A sketch of a cylindrical field map mesh, *i.e.*, a set of m(R, θ) nodes in a frame (O, X, Y), covering 180^0 (solid lines). The median plane field map so defined, namely the set of vertical field component values $B_Z(R, \theta)$ at the nodes of the mesh, represents a half of the cyclotron dipole; using it twice (additional 180^0 dashed line mesh) allows covering the all 360º dipole. The mesh nodes are distant ΔR radially, $\Delta \theta$ in angle. Note: fabricating a 2D median plane field map is an easy way to define a magnetic field distribution for raytracing, often useful when an accurate analytical modeling is not available at hand.

 • **Exercise 1.1-1.** *Model a magnet using a field map; raytrace using that field map model; check geometrical and dynamical outcomes against theory.*
Note 1: The optical sequence in zgoubi, for this exercise, is given in appendix 1.5.1
It uses (see *Zgoubi Users's Guide*), (i) OBJET to define a reference rigidity and to define the initial particle coordinates; (ii) TOSCA to read the field map and track

4   *Cyclotron*

through step-by-step (and `TOSCA`'s 'IL=2' flag to store step-by-step particle data into zgoubi.plt); (iii) `FAISCEAU` to print out particle coordinates in zgoubi.res, or `FAISTORE` to print out in *e.g.* zgoubi.fai.

Note 2: A short fortran program that generates the 180° field map needed, is given in App. 1.5.1.

a - Construct a 180-degree 2-dimensional map of the field $B(R, \theta)$ in the plane located half-way between the north and south poles in Fig. 1.5. (the "median plane"). Use a uniform mesh in a cylindrical coordinate system (R, θ), covering R=1 to 76 cm. Zgoubi requires a reference radius as part of the field map data, a convenient value is $R_M = 50$ cm. The radial increment of the mesh is $\Delta R = 0.5$ cm, the axial increment is $\Delta \theta = 0.5$ cm/RM. Take constant axial field B = 0.5 T. The storage file, to be read by the tracking code, will have the following formatting, 6 columns:

$$R \cos \theta, \ Z, \ R \sin \theta, \ BY, \ BZ, \ BX$$

with θ varying first, R varying second in that list. Z is the vertical direction (normal to the map mesh), $Z \equiv 0$.

b - Compute trajectories: for one turn, track a few protons on concentric trajectories centered on the center of the field map, ranging in $10 \leq R \leq 80$ cm (radius R and particle momentum $p = qB\rho$ shall have proper correlation for that, to be determined). Plot these concentric trajectories in the lab frame.

c - Plot the revolution time T_{rev} as a function of radius R and kinetic energy E_k (two abscissa axes). Superimpose the theoretical $T_{rev}(R)$ and $T_{rev}(E_k)$ curves. Explain what causes the slow increase of revolution period with energy. •

The difference between static field (conservative, *e.g.*, Cockcroft-Walton's) and time-varying field (non-conservative, cyclotron's - resonant) acceleration mechanisms:

It is not possible to accelerate a particle traveling on a closed path using an electrostatic field ($\tilde{E} = -\widetilde{\text{grad}}V(\tilde{R}, t)$ derives from a scalar potential), as the work by $\vec{F} = q\vec{E}$ only depends on the initial and final states, it does not dependent on the path followed (Fig. 1.8):

$$W = \int_A^B \vec{F}.d\vec{s} = -q \int_A^B \vec{\text{grad}}V.d\vec{s} = -q(V_B - V_A).$$

On a closed path : $\oint \vec{F}.d\vec{s} = 0$, conservative force, no work performed   (1.1)

Consequence: a DC voltage gap in a circular machine does not yield energy gain. Instead, the work of a force of induction origin ($\tilde{E} = -\partial \tilde{A}/\partial t$ arises from the variation of a magnetic flux - $\tilde{B} = \widetilde{\text{rot}}\tilde{A}$, $\tilde{A}$ vector potential) may not be null on a closed path. This is achieved *for instance* using a radio-frequency system which feeds an oscillating voltage across a gap, $\hat{V}\sin(\omega_{rf}t + \phi)$ (Fig. 1.9). In the classical cyclotron the gap is formed mechanically by a double dee system (Fig. 1.5). In the separated sector cyclotron (Fig. 1.2) the accelerating system is an external resonant cavity inserted in the drift space between two magnets (in a similar manner as today's synchrotrons).

The quantities of concern, regarding orbital motion (R, $f_{rev} = \omega_{rev}/2\pi$), field
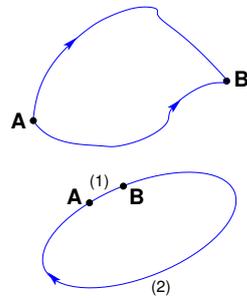
Fig. 1.8   The work of the electrostatic force only depends on V_A and V_B, independent of the path. In the case of the closed path: the particle loses along (2) the energy gained along (1).
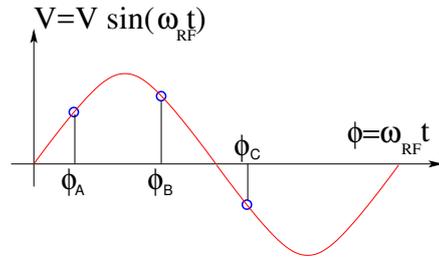

Fig. 1.9   A particle which reaches the gap at $\omega_{\mathrm{rf}}\mathrm{t} = \phi_A$ or $\omega_{rf}t = \phi_B$ is accelerated. If it reaches the RF gap at $\omega_{\mathrm{rf}}\mathrm{t} = \phi_C$ it is decelerated.

(B), satisfy

$$\mathrm{BR} = \mathrm{p/q}, \qquad 2\pi\mathrm{f_{rev}} = \mathrm{v/R} = \mathrm{qB/m} \qquad (1.2)$$

These relationships hold whatever γ, from $v \ll c$ ($\gamma \approx 1$, domain of the *classical* cyclotron technology) to $\gamma > 1$ (domain of the *isochronous* cyclotron technology).

Note the first quantity introduced above, the *rigidity* of the particle of charge q and momentum p, $\mathrm{BR} = \mathrm{p/q}$, with R the curvature radius of the trajectory under the effect of the Laplace force in the field B. The *particle rigidity* is a quantity of predilection in accelerator physics and design, it will be omnipresent along these lectures.

The RF frequency $\mathrm{f_{rf}} = \omega_{\mathrm{rf}}/2\pi$ is constant in a cyclotron. In the isochronous cyclotron it satisfies $\mathrm{f_{rf}} = \mathrm{hf_{rev}}$ at a great accuracy, at all time (Sec. 1.3.3). In the classical cyclotron $\mathrm{f_{rf}}$ is set, by design, equal to $\mathrm{hf_{rev}}$ for an intermediate energy during the acceleration cycle, as the revolution time does vary (decreases) (Sec. 1.2.4).

The energy gain, or loss, by the particle when transiting the gap is

$$\Delta\mathrm{W} = \mathrm{q}\hat{\mathrm{V}}\sin\phi(\mathrm{t}) \quad \text{with } \phi(\mathrm{t}) = \omega_{\mathrm{rf}}\mathrm{t} - \omega_{\mathrm{rev}}\mathrm{t} + \phi_0 \qquad (1.3)$$

with ϕ its phase with respect to the RF signal at the gap (*e.g.*, ϕ_A, ϕ_B or ϕ_C in Fig. 1.9) and ϕ_0 the value at $t = 0$, $\omega_{\mathrm{rev}}\mathrm{t}$ the orbital angle of the particle.

• Exercise 1.1-2. *Modeling an accelerating gap, acceleration in a cyclotron.*
Using the earlier 180° field map and zgoubi input file, introduce an accelerating gap with peak voltage $100\,\mathrm{kV}$: simulate it by means of `CAVITE[IOPT=3]`, and reproducing the configuration of Fig. 1.6.
a - Inject a proton with starting kinetic energy $200\,\mathrm{keV}$ (at the appropriate starting radius, $\mathrm{R_0} = \mathrm{p_0/qB}$, to be determined). Let it accelerate turn-by-turn through the gap (for multiturn, use `REBELOTE[NPASS=as many turns as needed; K=99]`, placed at the end of the sequence) until it reaches $6\,\mathrm{MeV}$ kinetic energy about. Plot the accelerated (spiraling out) trajectory all the way in a similar $(\mathrm{O, X, Y})$ frame as in Fig. 1.7 (step-by-step particle data can be read from zgoubi.plt).
b - Plot the proton momentum pc and total energy E as a function of its kinetic energy, both from this numerical experiment (raytracing data stored using `FAISTORE`)

6   *Cyclotron*

and from theory, everything on the same graph, use MeV units.

c - Plot the normalized velocity $\beta = v/c$ as a function of kinetic energy, both numerical and theoretical, and in the latter case both classical and relativistic. ● **c -** Plot

the relative change in velocity $\Delta v/v$, as well as the relative change in circumference $\Delta \mathcal{C}/\mathcal{C}$, as a function of kinetic energy. both numerical and theoretical. From their evolution, conclude that the time of flight decreases with energy. ●

● **Exercise 1.1-3.** *Accelerating to high energy, relativistic dynamics.*
Push the previous exercise to $3\,\mathrm{GeV}$ kinetic energy. For that, it will be necessary to extend the field map, to a maximum radius proper to encompass the spiraling trajectory up to $3\,\mathrm{GeV}$. ●

● Exercise 1.3-1. Some useful relationships for the sequel. Demonstrate the following:
$\frac{dp}{p} = \frac{1}{\beta^2}\frac{dE}{E}; \quad \frac{d\beta}{\beta} = \frac{1}{\gamma^2}\frac{dp}{p} = \frac{1}{\beta^2\gamma^2}\frac{dE}{E}; \quad \frac{d\gamma}{\gamma} = \frac{dW}{m_0+W}$ (W = kinetic energy); $\frac{dW}{W} = \frac{\gamma+1}{\gamma}\frac{dp}{p}$. ●

1.2   Classical cyclotron

Fixed-frequency acceleration requires the RF and cyclotron frequencies to be matched to one another. However the relativistic increase of the mass upon acceleration causes the revolution period to decrease with momentum, at a turn-by-turn rate of $\Delta T/T_{\mathrm{rev}} = 1 - \gamma$. Revolution time decreases - revolution frequency increases - while the ion spirals out.

● **Exercise.**   Give a theoretical demonstration of that relationship. ●

The mis-match between the accelerating and cyclotron frequencies is a turn-by-turn cumulative effect and sets a limit to the highest velocity, $\beta = v/c \approx 0.22$, $\Delta T/T_{\mathrm{rev}} \approx 2 - 3\%$. This will be addressed in Sec. 1.2.4. For the time being: this means for instance a limit of applicability of the "classical cyclotron" in the region $E - mc^2 \lesssim 25\,\mathrm{MeV}$ for protons, $\lesssim 50\,\mathrm{MeV}$ for D and α particles.

1.2.1   *Fixed-energy orbits, revolution period*

● **Exercise 1.2.1-1.** *Numerical convergence of the integration method: field model and integration step size.*
In view of the exercises in the next sections, we will work from now on with a 60° sector dipole (thus 6 setors are needed to model the cyclotron).
a - Compute the field map of a 60° sector, with the same mesh density as used in Ex. 1.1: radial increment of the mesh $\Delta R = 0.5\,\mathrm{cm}$, axial increment $\Delta\theta = 0.5\,\mathrm{cm/RM}$ (the fortran program in App. 1.5.1 can be used again).
- Check the evolution of the cyclotron orbit radius and revolution period with field map mesh density, namely, compute a second field map with increments ΔR and

$\Delta\theta$ twice as large; plot the orbit radius R and revolution time T_{rev} as a function of the kinetic energy E_k (say, $E_k : 1 \to 5\,\mathrm{MeV}$) in both cases. Repeat with additional field maps with decreasing mesh density, until noticeable changes to these curves are observed. Add on the graph the theoretical curves for R and T_{rev}. Note: a possibility for better assessing the effect of changing the mesh density is, instead, plotting the relative difference $\delta R/R$ and $\delta T_{rev}/T_{rev}$.
- With the denser mesh map (more accurate field modeling) check the effect of the integration step size on these quantities: plot the orbit radius R and revolution time T_{rev} (or the relative difference $\delta R/R$ and $\delta T_{rev}/T_{rev}$) as a function of the kinetic energ E_k, for a few step size values ranging in $1\,\mathrm{mm}-2\,\mathrm{cm}$, all on the same graph.

b - Use instead Zgoubi's `DIPOLE` analytical modeling for the field over a 60° sector: no more field map here, the field at the location of the particle is computed from an analytical model, at each integration step. Re-do the step-size test above. Note : The optical sequence for this exercise is given in appendix 1.5.2.

c - From the two series of results, comment on various pros and cons of the two methods, analytical field models and field maps. •

Periodic motion - Horizontal motion in a uniform field cyclotron has no privileged reference orbit: for a given momentum, the initial radius and velocity vector define a particular closed, circular orbit. A particle launched with an axial velocity component on the other hand, drifts vertically linearly with time, as there is no axial restoring force (the field is normal to the horizontal plane). The next Section will investigate the necessary field property, absent in our simplified field model so far, proper to ensure confinement of the multiturn periodic motion in the vicinity of the median plane of the cyclotron dipole magnet.

• Exercise 1.2.1-2. *Observe the two statements above.*
a - First statement: plot trajectories of particles launched with different initial velocity vector (and zero axial velocity component) over one turn. Give their theoretical parametric equation in a Cartesian frame (O;X,Y) centered at the center O of the cyclotron; superimpose with numerical trajectories (the option `IL=2` in `TOSCA` can be used to store particle coordinates through the field maps, step-by-step).
b - Second statement: plot the axial motion of a particle launched with a non-zero initial axial velocity component. Give its theoretical vertical position Z(s) (Z is along the Lab. vertical axis, s is the path length); superimpose with the numerically computed trajectory. •

• Exercise 1.2.1-3. *Unstable motion in uniform field.*
a - Plot two particle trajectories that demonstrate the value of the radial wave number in a uniform field. Conclude on the orbit and on horizontal motion stability.
b - Derive the horizontal and axial transport matrices from raytracing (use `MATRIX[IFOC=11]`, placed in sequence with the optical sequence). Conclude on the stability of charged particle motion in a uniform field. •

1.2.2 *Weak focusing*

In the following, $B_R(R)$, $B_y(R)$ are respectively the radial and axial components of the magnetic field at R. Median-plane symmetry of the field is assumed, so that $B_R|_{y=0} = 0$ at all R (Fig. 1.10-right).

• Exercise. Show that the mid-plane symmetry hypothesis results in $B_R|_{y=0} = 0$. •

Introduce the small radial distance

$$x(s) = R(s) - R_0 \ll R_0 \tag{1.4}$$

from a reference radius R_0 (with center the center of the axially symmetric cyclotron magnet, Fig. 1.10). The radial and axial forces experienced by a particle at x write, to the first order in the radial and axial coordinates, respectively x and y,

$$F_x = m\ddot{x} = -qvB_y(R) + m\frac{v^2}{R_0 + x} \approx -qv\left(B_y(R_0) + \frac{\partial B_y}{\partial R}\bigg|_{R_0} x\right) + m\frac{v^2}{R_0}\left(1 - \frac{x}{R_0}\right)$$

$$F_y = m\ddot{y} = qvB_R(R) = qv\,\frac{\partial B_R}{\partial y}\bigg|_{y=0} y + \text{higher order} \approx qv\frac{\partial B_y}{\partial R}y \tag{1.5}$$

Note the following two steps in deriving these expressions:
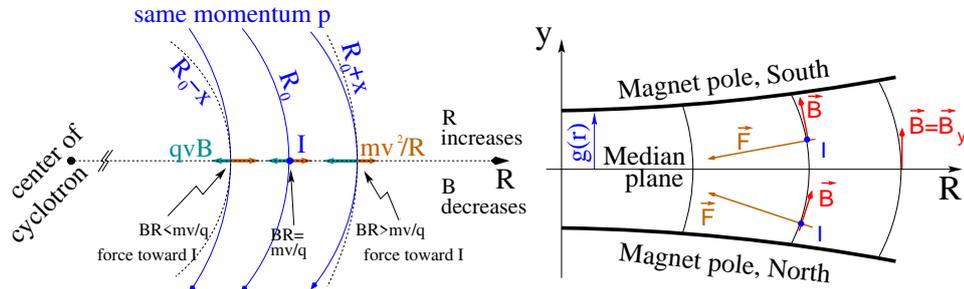
Fig. 1.10   Motion stability in a weak focusing axially symmetric structure. Left, radial: the resultant of the bending and outward forces pulls particles with momentum p = mv toward the equilibrium orbit at $R_0 = p/qB_0$, resulting in a stable oscillation around the latter. Right, axial: positive ions off the median plane (at I, coming out of the page) experience a force pulling toward the median plane.

- the force F_x which applies on the ion is the resultant of the pseudo force $f_c = m\frac{v^2}{R}$, oriented away from the center of the motion, and of the magnetic force $f_B = -qvB_y(R)$, oriented toward the center of the motion. In particular, $-qvB_y(R_0) + m\frac{v^2}{R_0} = 0$.
- a Taylor expansion of the magnetic field yields a first order expression of the r-dependence,

$$B_y(R_0 + x) = B_y(R_0) + x\,\frac{\partial B_y}{\partial R}\bigg|_{R_0} + \frac{x^2}{2!}\,\frac{\partial^2 B_y}{\partial R^2}\bigg|_{R_0} + ... \approx B_y(R_0) + x\,\frac{\partial B_y}{\partial R}\bigg|_{R_0}$$

The relations Eq. 1.5 yield the differential equations for the radial and axial motions, respectively,

$$\ddot{x} + \omega_R^2 x = 0 \qquad \text{and} \qquad \ddot{y} + \omega_y^2 y = 0 \tag{1.6}$$

wherein

$$\omega_R^2 = \omega_{rev}^2 (1 + \frac{R_0}{B_0} \frac{\partial B_y}{\partial R}), \quad \omega_y^2 = -\omega_{rev}^2 \frac{R_0}{B_0} \frac{\partial B_y}{\partial R} \tag{1.7}$$

noting $B_y(R_0) = B_0$, and with $\omega_{rev} = 2\pi f_{rev}$ the angular frequency of the circular motion. Focusing by a restoring force appears (Eq. 1.6) owing to the use of a magnetic field with radial index

$$k = \frac{R_0}{B_0} \frac{\partial B_y}{\partial R}|_{R=R_0, y=0} \tag{1.8}$$

Radial stability in an axially symmetric structure with weakly decreasing field $B(R)$ is sketched in Fig. 1.10-left : At larger motion radius, $R > R_0$ (resp. smaller, $R < R_0$), a particle with momentum $p = mv$ (assumed charged positively) experiences a decrease (resp. increase) of the outward force $f_c = m\frac{v^2}{R}$ at a higher rate than the decrease (resp. increase) of the bending force $f_B = -qvB$. In other words, radial stability requires BR to be an increasing function of R, $\frac{\partial BR}{\partial R} = B + R\frac{\partial B}{\partial R} > 0$, this holds in particular at R_0 thus $1 + k > 0$.

Axial stability requires a restoring force directed toward the median plane, $F_y = -ay < 0$, , thus $B_R = -by < 0$, a guiding field decreasing with radius, Fig. 1.10-right. With $\partial B_y/\partial r = \partial B_R/\partial y$ this means $k < 0$.

The resulting condition of motion stability around the equilibrium orbit

$$-1 < k < 0 \tag{1.9}$$

The two quantities in Eq. 1.7

$$\nu_R = \omega_R/\omega_{rev} = \sqrt{1+k}, \quad \nu_y = \omega_y/\omega_{rev} = \sqrt{-k} \tag{1.10}$$

are known as the "wave numbers" (or "tunes"), respectively radial and axial, the number of oscillations of the particle about the reference circular orbit of radius R_0. Note that there is less than an oscillation per revolution and in addition

$$\nu_R^2 + \nu_y^2 = 1 \tag{1.11}$$

● Exercise 1.2.2-1. *Introducing a radial field index.*
Constant field-gradient focusing ($\partial B/\partial R$=constant over the useful field region) stems from a linear decrease of the magnetic field with radius - distance to the center of the cyclotron (this can be realized practically with the gap slowly opening up, linearly with radius).

a - Use `TOSCA` and the 60° sector field map of exercise 1.2.1-1, construct the sector field map accounting for a radial index k: take the 200 keV injection radius R_0 as the reference radius in this exercise (R_0 is required to define the index k, Eq. 1.8). Track that 200 keV orbit, plot it in the lab frame: make sure it comes out as expected, namely, constant radius, final and initial angles equal (normally null given the working hypotheses established in the previous exercises).

b - Find the orbit radius $R(B\rho)$ numerically, for a series of $B\rho$ values such to cover the extent of the field map (use the `FIT` procedure to find R for a given particle rigidity and `REBELOTE` to repeat); plot both numerical and theoretical $B\rho(R)$ (use `FAISTORE` storage command placed between `FIT` and `REBELOTE`).

c - Plot the axial paraxial motion of a $1\,\mathrm{MeV}$ proton, over a few turns (use as earlier, `IL=2` under `TOSCA` and the data so logged to zgoubi.plt). Check the effect of the focusing strength by comparing the trajectories for a few different index values, including close to -1 or close to 0.

d - Plot the magnetic field experienced by the particle along these trajectories. •

• Exercise 1.2.2-2. *A radial field index in* `DIPOLE`.
Introduce a radial field index, using the analytical modeling `DIPOLE`. A template input file to Zgoubi is guven in App. 1.5.2.
Repeat questions a to d of exercise 1.2.2-1. •

Isochronism - The focusing condition $-1 < \mathrm{k} < 0$ breaks the isochronism as it causes the guiding field B and thus $\omega_{\mathrm{rev}} = \mathrm{qB/m}$ to change (decrease) with R. As a consequence, the arrival time of a particle at the RF gap (by extension the "RF phase" of the motion) is not constant (this is addressed in Sec. 1.2.4).

1.2.3   *Coordinate transport*

Introducing the path variable, s, as the independent variable in Eq. 1.6 and using the approximation $\mathrm{ds} \approx \mathrm{vdt}$, Eqs. 1.6 take the form

$$\frac{\mathrm{d}^2\mathrm{x}}{\mathrm{ds}^2} + \frac{1+\mathrm{k}}{\mathrm{R}_0^2}\mathrm{x} = 0, \qquad \frac{\mathrm{d}^2\mathrm{y}}{\mathrm{ds}^2} - \frac{\mathrm{k}}{\mathrm{R}_0^2}\mathrm{y} = 0 \tag{1.12}$$

The solutions write, for respectively the horizontal and vertical motions,

$$\begin{cases} \mathrm{R(s)} - \mathrm{R}_0 = \mathrm{x(s)} = \mathrm{x}_0 \cos\frac{\sqrt{1+\mathrm{k}}}{\mathrm{R}_0}(\mathrm{s}-\mathrm{s}_0) + \mathrm{x}_0'\frac{\mathrm{R}_0}{\sqrt{1+\mathrm{k}}}\sin\frac{\sqrt{1+\mathrm{k}}}{\mathrm{R}_0}(\mathrm{s}-\mathrm{s}_0) \\ \mathrm{R'(s)} = \mathrm{x'(s)} = \quad -\mathrm{x}_0\frac{\sqrt{1+\mathrm{k}}}{\mathrm{R}_0}\sin\frac{\sqrt{1+\mathrm{k}}}{\mathrm{R}_0}(\mathrm{s}-\mathrm{s}_0) + \mathrm{x}_0'\cos\frac{\sqrt{1+\mathrm{k}}}{\mathrm{R}_0}(\mathrm{s}-\mathrm{s}_0) \end{cases} \tag{1.13}$$

$$\begin{cases} \mathrm{y(s)} = \quad \mathrm{y}_0 \cos\frac{\sqrt{-\mathrm{k}}}{\mathrm{R}_0}(\mathrm{s}-\mathrm{s}_0) + \mathrm{y}_0'\frac{\mathrm{R}_0}{\sqrt{-\mathrm{k}}}\sin\frac{\sqrt{-\mathrm{k}}}{\mathrm{R}_0}(\mathrm{s}-\mathrm{s}_0) \\ \mathrm{y'(s)} = -\mathrm{y}_0\frac{\sqrt{-\mathrm{k}}}{\mathrm{R}_0}\sin\frac{\sqrt{-\mathrm{k}}}{\mathrm{R}_0}(\mathrm{s}-\mathrm{s}_0) + \mathrm{y}_0'\cos\frac{\sqrt{-\mathrm{k}}}{\mathrm{R}_0}(\mathrm{s}-\mathrm{s}_0) \end{cases} \tag{1.14}$$

• Exercise 1.2.3-1.   *Projected particle trajectories.*
Use `DIPOLE` preferably (rather than `TOSCA`) for greater accuracy. No acceleration in this exercise (if present in the sequence, `CAVITE` is turned off, or commented), particles run around at constant energy.

a - Plot the horizontal and vertical trajectory components x(s) and y(s) of a particle with rigidity close to $\mathrm{B}\rho(\mathrm{R}_0)$ (R_o is the reference radius in the definition of the index k), over a few turns around the cyclotron. From the number of turns, give an estimate of the wave numbers. Check the agreement with the expected $\nu_\mathrm{R}(\mathrm{k})$, $\nu_\mathrm{y}(\mathrm{k})$ values from Eq. 10 in the course. Take particle energy $1\,\mathrm{MeV}$ instead, which is far from kinetic-$\mathrm{E}(\mathrm{R}_0)$; the wave numbers change: could that be expected? Explain.

b - In the former case, $200\,\mathrm{keV}$ energy, plot as a function of s the difference between x(s) from tracking and its values from Eq. 1.13. Same for y(s) compared to Eq. 1.14. Is there agreement? (use the option `IL=2` to store particle coordinates in zgoubi.plt, step-by-step). •

Note that the dissymmetry between the conditions of horizontal stability (term "1" in "$\sqrt{1+k}$") and vertical stability ("$\sqrt{-k}$") arises from the focusing introduced by the curvature, a purely geometrical effect. The focal distance associated with the curvature of a magnet of arc length $\mathcal{L}$ is obtained by integrating $\frac{d^2x}{ds^2} + \frac{1}{R_0^2}x = 0$ and identifying with the focusing property $\Delta x' = -x/f$, namely,

$$\Delta x' = \int \frac{d^2x}{ds^2} ds \approx \frac{-x}{R^2} \int ds = \frac{-x\mathcal{L}}{R^2}, \quad \text{thus} \quad f = \frac{R^2}{\mathcal{L}}$$

● Exercise 1.2.3-2.   *Phase space motion, Fourier analysis.*
Track a particle with small amplitude radial and axial motions (paraxial motion) with respect to the reference circular closed orbit, at constant energy, in a cyclotron based on the earlier material.
a - At some azimuth s around the ring, observe the coordinates (x(n),x'(n)) of a particle as it circles around for many turns (n is the turn number) (use `FAISTORE` to store particle coordinates in zgoubi.fai, turn after turn). Plot (x(n),x'(n)) in the "transverse phase-space", (x,x'). Using the trajectory Eq. 1.13 show that the particle trajectory in phase space is on an ellipse and calculate the ellipse parameters. Verify that it superposes on the particle motion in the graph.
b - Compute the radial and axial wave numbers by Fourier analysis of respectively the x(n) and the y(n) motion. There is an indetermination on the value of the wave number, explain. Check the agreement with the expected $\nu_R(k)$, $\nu_y(k)$ values from Eq. 10 in the course. ●

Chromatism, chromatic orbit -   In an axially symmetric structure, the equilibrium trajectory at momentum $\begin{cases} p_0 \\ p_A \end{cases}$ is at radius $\begin{cases} R_0 \text{ such that } B_0R_0 = p_0/q \\ R_A \text{ such that } B_AR_A = p_A/q \end{cases}$,

with $\begin{cases} B_A = B_0 + \left(\frac{\partial B}{\partial x}\right)_0 + ... \\ R_A = R_0 + \Delta x \\ p_A = p_0 + \Delta p, \end{cases}$

On the other hand

$B_AR_A = \frac{p_A}{q} \text{Rightarrow} \left[B_0 + \left(\frac{\partial B}{\partial x}\right)_0 \Delta x + ...\right][R_0 + \Delta x] = \frac{p_0 + \Delta p}{q} = \frac{p_0}{q} + \frac{\Delta p}{q}$

and, neglecting terms in $(\Delta x)^2$: $B_0R_0 + \left(\frac{\partial B}{\partial x}\right)_0 R_0\Delta x + B_0\Delta x = \frac{p_0}{q} + \frac{\Delta p}{q}$, which, given $B_0R_0 = \frac{p_0}{q}$, leaves $\Delta x \left[\left(\frac{\partial B}{\partial x}\right)_0 R_0 + B_0\right] = \frac{\Delta p}{q}$, which given $n = -\frac{R_0}{B_0}\left(\frac{\partial B}{\partial x}\right)_0$ yields

$$\Delta x = \frac{R_0}{1+k}\frac{\Delta p}{p_0} = D\frac{\Delta p}{p_0} \tag{1.15}$$

In passing we have introduced the quantity $D = \frac{R_0}{1+k}$, the "dispersion" factor with respect to the reference closed orbit at R_0. This establishes that, when R_0 or k are s-dependent quantities (as in the synchrotron, next Chapters), D(s) is the solution of the differential equation

$$\frac{d^2D(s)}{ds^2} + \frac{1+k}{R_0^2}D(s) = \frac{1}{R_0} \tag{1.16}$$

However D is a constant in the present case of the non-relativistic cyclotron (k is constant by definition, and $R_0 = p_0/qB_0$ is constant).
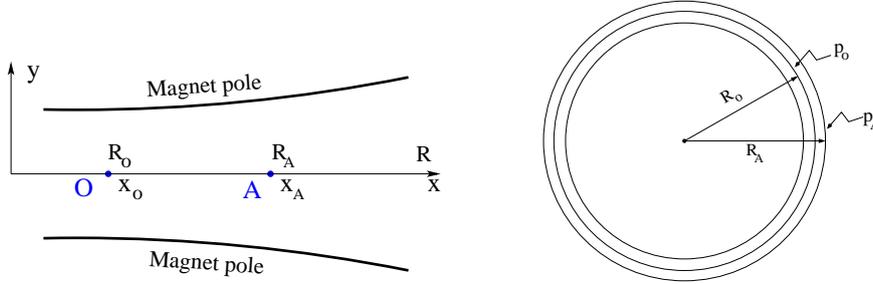
Fig. 1.11   The equilibrium radius at location $O(x = x_0)$ is $R = R_0$, the equilibrium momentum is p_0, rigidity $BR = B_0R_0$. The equilibrium radius at $A(x = x_A)$ is $R = R_A$ for the particle with momentum $p_A = p_0 + \Delta p$, rigidity $BR = B_AR_A$.

1.2.4 *Resonant acceleration*

An oscillating radio-frequency (RF) electric field, with fixed-frequency f_{rf} is applied in the gap between the two dees (Fig. 1.5). An ion of charge q reaching the gap at time t undergoes a change in energy

$$\Delta W(t) = q\hat{V} \sin \phi \quad \text{with } \phi = \omega_{rf}t - (\omega_{rev}t + \phi_0) \tag{1.17}$$

with ϕ the RF phase experienced by the particle at the time it crosses the gap and ϕ_0 the origin in phase for the particle motion (normally about $\pi/2$, in the region of the crest of V(t) oscillation). Note that this ignores the "transit time", the effect of the time that the particle spends across the gap on the overall energy gain; focusing in the cyclotron, in what follows, will ignore as well the effect of the electric gap.

The frequency dependence of the kinetic energy W of the ion relates to its orbital radius R in the following way:

$$W = \frac{1}{2}mv^2 = \frac{1}{2}m(2\pi Rf_{rev})^2 \approx \frac{1}{2}m(2\pi R\frac{f_{rf}}{h})^2 \tag{1.18}$$

thus, for a given cyclotron size (R), f_{rf} and h set the limit for the acceleration range.

The revolution time/frequency increases/decreases with energy and the condition of synchronism with the oscillating voltage, $f_{rf} = hf_{rev}$, is only fulfilled at one particular radius in the course of acceleration (Fig. 1.12). To the left and to the right, out-phasing $\Delta\phi$ builds-up turn after turn, decreasing in a first stage (towards zero, $\phi < \pi/2$ and lower voltages, Fig. 1.12-right) and then increasing back to $\phi = \pi/2$ phase and beyond towards $\phi = \pi$ - the boundary for the acceleration mode.

Differentiating the particle phase at the RF gap, over a half-turn (Eq. 1.17 with ω_{rev} constant between two gaps) one gets $\dot{\phi} = \omega_{rf} - \omega_{rev}$. Over a half-turn in addition, $\Delta\phi = \dot{\phi}\frac{\pi R}{v}$, yielding a phase-shift per half-turn of

$$\Delta\phi = \pi \left(\frac{m\omega_{rf}}{qB} - 1 \right) \tag{1.19}$$

Due to this cumulative out-phasing the classical cyclotron requires quick acceleration (limited number of turns), which means high voltage (tens or hundreds of kVolts). As expected, with ω_{rf} and B constant, $\Delta\phi$ presents a minimum ($\dot{\phi} = 0$) at
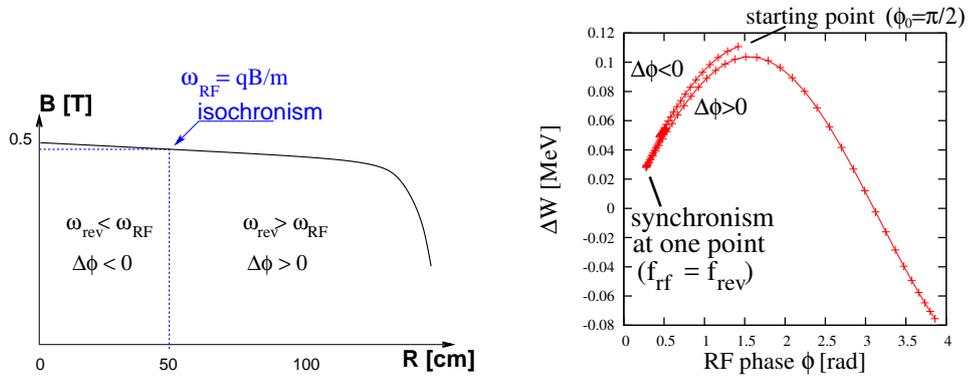
Fig. 1.12   Synchronous condition at one point (left), h=1 assumed here, and span in phase of the energy gain $\Delta W = q\hat{V} \sin\phi$ over the acceleration cycle (right). ϕ is the phase of the RF sine wave at arrival of the particle at the accelerating gap. Note that the vertical separation of the two $\Delta W(\phi)$ branches on the right ($\Delta\phi < 0$ and $\Delta\phi > 0$) is artificial, this is for clarity, they are actually superimposed.

$\omega_{\mathrm{rf}} = \omega_{\mathrm{rev}} = \frac{qB}{m}$ where exact isochronism is reached (Fig. 1.12). The upper limit to ϕ is set by the condition $\Delta W > 0$, acceleration.

• Exercise 1.2.4-1. *RF phase shift at the accelerating gap.*
Consider the cyclotron model of exercise 1.2.2-2 (which uses `DIPOLE` and a double accelerating gap). Take the following parameters: field index k = -0.03125, field $B_0 = 5\,\mathrm{kG}$ on injection radius, injection energy $W_0 = 200\,\mathrm{keV}$, peak gap voltage $\hat{V} = 100\,\mathrm{kV}$. Assume, first, that the acceleration is independent of the arrival phase (use `CAVITE[IOPT=3]`, at both gaps).
a - Track a proton from 1 to 5 MeV: get the turn-by-turn phase-shift at the gap, compare with Eq. 1.19.
**b -** Produce a similar diagram $\Delta W(\phi)$ to Fig. 1.12-right. •
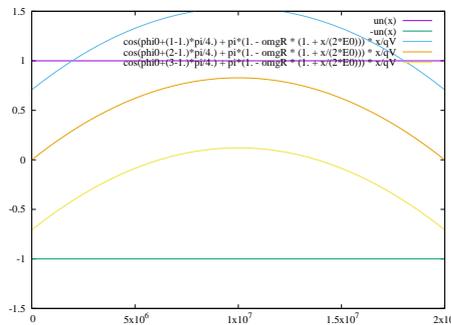
Fig. 1.13   The cyclotron equation.

• Exercise 1.2.4-2.   *The cyclotron equation*

14   *Cyclotron*

relates RF phase ϕ and particle energy E, it writes [6]

$$\cos\phi = \cos\phi_{\mathrm{i}} + \pi \left[1 - \frac{\omega_{\mathrm{rf}}}{\omega_{\mathrm{rev}}} \frac{\mathrm{E} + \mathrm{E_i}}{2\mathrm{E_0}} \right] \frac{\mathrm{E} - \mathrm{E_i}}{\mathrm{q}\hat{\mathrm{V}}} \tag{1.20}$$

(E=W+$\mathrm{E_0}$ =total energy, $\mathrm{E_0}$ =rest mass, index i denotes injection) and is represented in Fig. 1.13 for various values of RF phase at injection ϕ_{i}. The cyclotron model of exercise 1.2.4-1 may be used here.

a - In an attempt to accelerate over a kinetic energy range of about $[0.2, 20]\,\mathrm{MeV}$, assume maximum of $\cos(\phi)$ at $\mathrm{W_m} = 10\,\mathrm{MeV}$. From $\mathrm{d}(\cos\phi)/\mathrm{dW} = 0$ at $\mathrm{W_m}$, deduce the operation RF frequency (assume RF harmonic h=1).
Set up the Zgoubi model accordingly. **b -** Plot the theoretical energy-phase relationship characteristic of the cyclotron acceleration: for $\phi_0 = \frac{3\pi}{4}$, $\frac{\pi}{2}$, $\frac{\pi}{4}$, from both simulation and theory •

1.3 Relativistic cyclotron

The bad news with relativistic effects is that the particle slows down with energy and loses synchronism. From the cyclotron resonance $\omega_0 = \mathrm{qB}/\gamma\mathrm{m_0}$, given $\mathrm{R} = \beta\mathrm{c}/\omega_0$, one gets the particular relationship

$$\mathrm{k} = \frac{\mathrm{R}}{\mathrm{B}} \frac{\partial\mathrm{B}}{\partial\mathrm{R}} = \frac{\beta}{\gamma} \frac{\partial\gamma}{\partial\beta} = \beta^2\gamma^2 \tag{1.21}$$

Thus synchronism requires $\frac{\mathrm{R}}{\mathrm{B}}\frac{\partial\mathrm{B}}{\partial\mathrm{R}} = \mathrm{k}$ to be positive and increasing with energy: the weak focussing condition $-1 < \mathrm{k} < 0$ is not satisfied, transverse stability is lost.

Note also that, by constrast to the earlier weak-focusing conditions, k can no longer be a constant, it has to increase with R. Thus the wave numbers (Eq. 1.10) also change with R (in particular, the horizontal wave number follows γ, a consequence of the isochronism, this will be discussed later).

The revolution period on the equilibrium orbit, momentum p = qBR and circumference $\mathcal{C}$, is $\mathrm{T} = \mathcal{C}/\beta\mathrm{c} = 2\pi\gamma\mathrm{m_0}/\mathrm{qB}$. Isochronism requires p-invariant revolution period, $\mathrm{dT/dp} = 0$. Differentiating the previous expression, this requirement yields

$$\mathrm{B(R)} = \frac{\mathrm{B_0}}{\gamma_0}\gamma(\mathrm{R}) \tag{1.22}$$

with $\mathrm{B_0}$ and γ_0 free reference conditions, and the reference revolution period is noted $\mathrm{T_0}$. In other words, isochronism requires $\mathrm{B(R)} \propto \gamma$, and this yields axial defocusing.

H.A. Bethe and M.E. Rose once stressed [3] "... it seems useless to build cyclotrons of larger proportions than the existing ones... an accelerating chamber of 37 cm radius will suffice to produce deuterons of 11 MeV energy which is the highest possible...". Frank Cole : "If you went to graduate school in the 1940s, this inequality $[-1 < \mathrm{k} < 0]$ was the end of the discussion of accelerator theory."

Until...

1.3. Relativistic cyclotron   15

1.3.1   Thomas focusing

In 1938, L.H. Thomas introduces the concept of alternating regions of stronger and weaker axial field [4], the "AVF" (Azimuthally Varying Field) cyclotron (Fig. 1.14). The single-magnet concept of the classical cyclotron remains, however an azimuthal field modulation is introduced by shaping the magnet pole to create a $2\pi/N$-periodical field modulation. From this results a form factor, the "flutter", for instance of sinusoidal form

$$\mathcal{F}(\theta) \propto 1 + \mathrm{f}\sin(N\theta) \tag{1.23}$$

The necessary radial increase of the field for preserving the isochronism of the orbits in the relativistic regime (Eq. 1.22) is obtained by radial pole shaping. The median plane field now varies with both R and θ,

$$B(R, \theta) = B_0\,\mathcal{R}(R)\,\mathcal{F}(\theta) \tag{1.24}$$

Note that the orbit curvature is no longer constant along the orbit (which is no longer a circle) as a consequence of the AVF, for this reason a local curvature radius $\rho(s)$ is introduced in the following, in lieu of the former R assumed up to now constant over the 2π circular orbit. R instead will in general be used to denote the average radius of the closed, periodic orbit, $R = \oint ds/2\pi$.
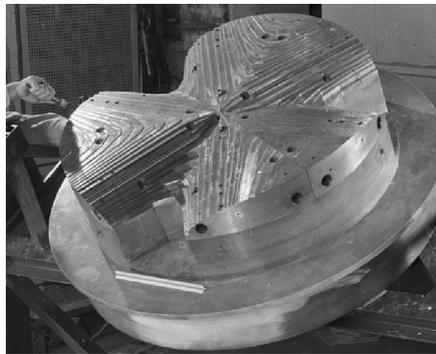
Fig. 1.14   Azimuthal pole shaping in Thomas-style AVF cyclotron.
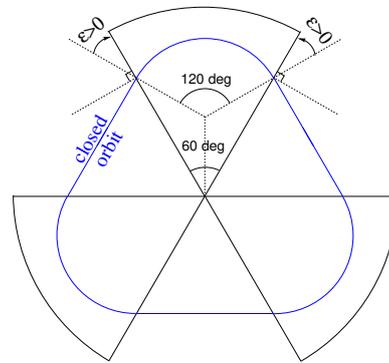
Fig. 1.15   Sketch of a 3-period, 120° sector, AVF cyclotron. The optical axis (or reference "closed orbit") is at $\epsilon = 30^o$ "wedge angle" with the sector dipole edge. The wedge is closing, it causes vertical focusing and weakens the horizontal focusing.

1.3.2   Spiral sector

In 1954 Kerst introduces a method for vertical wedge focusing which compensates for the radially increasing field gradient: by spiraling the edges of the sector dipoles (Fig. 1.3)

$$B(R, \theta) = B_0\,\mathcal{F}(R, \theta)\,\mathcal{R}(R), \quad \mathcal{F}(R, \theta) = 1 + \mathrm{f}\sin(N(\theta - \tan(\xi)\ln(R/R_0))) \tag{1.25}$$

16   *Cyclotron*

$R = R_0 \exp(\theta/\tan(\xi))$ is the equation of the spiral, centered at the center of the ring. This results in a larger contribution of the flutter term in the vertical wave number,

$$\nu_{\mathrm{y}} = \sqrt{-\mathrm{k} + \mathrm{F}^2(1 + 2\tan^2\xi)} \tag{1.26}$$

with ξ the spiral angle: the angle that the tangent to the spiral edge does with the ring radius.

In the late 1950s appeared the "separated sector cyclotron", in which the sector dipoles are separated by iron-free spaces (not really field-free, though, due the the field fall-offs) (Fig. 1.2). Isochronous cyclotrons nowadays still rely on these various principles and techniques, their limit in energy resides in achievable field strength, magnet size, and beam separation at the last turn for extraction.

Nowadays most isochronous cyclotrons over 40 MeV use spiral sectors [4.b], profiting from the strong effect of the term $2\tan^2\xi$). For instance, $\xi \leq 70^o$ in TRIUMF H- 520 MeV cyclotron, $\xi \leq 35^o$ in PSI 500 MeV proton cyclotron.

An instance of a single-magnet spiral sector AVF cyclotron is PSI's 250 MeV protontherapy machine, Fig. 1.3, the field at the center of the cyclotron is 2.4 T. An instance of a separated spiral sector cyclotron is PSI's 590 MeV, Fig. 1.2.

Simulations regarding spiral sector optics will be performed in the FFAG chapter.

1.3.3   *Isochronous acceleration*

Simualtions using a model of the PSI cyclotron (Fig. 1.2) are provided in a separate document, to be found in the CASE web site.

1.3.4   *Cyclotron extraction*

● **Exercise 1.3.4.** *Limit in energy.*
It follows from qBR = p that $\frac{\Delta\mathrm{R}}{\mathrm{R}} = \frac{***}{***}$. With $***$ the energy gain per turn this yields $\Delta\mathrm{R} = \frac{\mathrm{m}\Delta\mathrm{E_k}}{\mathrm{q}^2\mathrm{B}^2\mathrm{R}}$: the radius increment $\Delta\mathrm{R}$ decreases with R. As the extraction at the last turn requires sufficient separation from the last but one turn, for insertion of a deflector electrode (see Fig. 1.5), there is a practical feasibility limit. Plot the accelerated spiral, or the fixed-energy orbits, to top energy, observe this property. Plot dR(R), from both tracking and theory. ●

1.4   summary

In this Chapter the following has been addressed:

   - the uniform field (single-magnet) classical cyclotron, field characterized by B(θ) =constant,

   - weak transverse focusing, in both planes simultaneously, obtained by a slow radial decrease of the field, $\mathrm{B(R)} = \mathrm{B_0} + \mathrm{k}\frac{\mathrm{B_0}}{\mathrm{R_0}}(\mathrm{R} - \mathrm{R_0}), \quad -1 < \mathrm{k} < 0,$

   - near-crest, quasi-isochronous, resonant acceleration in the classical cyclotron, its limit in energy,

- Thomas "AVF" isochronus cyclotron; azimuthal field modulation ("flutter") and vertical focusing, with for instance $B(\theta) \propto B_0(1 + f\sin(3\theta))$,

- wedge focusing, enhanced vertical focusing by spiraling the pole edges,

- the isochronous cyclotron, a separated sector ring accelerator,

- relativistic resonant acceleration in an isochronous cyclotron.

Various notions and quantities which characterize charged particle dynamics in accelerators have been introduced, including:

- closed orbit,

- focusing and field index,

- differential equations of the motion, and their periodic solutions,

- wave numbers, motion invariant,

- dispersion function,

- transport of particle coordinates,

- transport matrix formalism.

18   *Cyclotron*

1.5   Appendix

1.5.1   *Field map and optical sequence for Exercise 1.1-1*

The cyclotron is defined using a 180° field map twice. This optical sequence can be copy-pasted to a Zgoubi input data file and run as it is, once the magnetic field map has been built (and saved in "geneSectorMap.out").

Consult zgoubi users' guide for the functionning of the various keywords (`OBJET`, `PARTICUL`, `FAISTORE`, `TOSCA`, `FAISCEAU`, `END`) and their subsequent data list.

Fortran program that generates a field map

This program builds a 180° magnetic field map in the appropriate format for zgoubi's `TOSCA [IX=315,IY=121,IZ=1,MOD=22]` field map reading mode. Save it in "geneSectorMap_180deg.out" for this exercise.

```
      implicit double precision (a-h,o-z)
      parameter (pi = 4.d0*atan(1.d0))

C------------ Hypothesis :
C Total angle extent of the field map. Can be changed, e.g., to 360, Or 60 deg, or else.
C     AT = 360.d0  /180.d0*pi
      AT = 180.d0  /180.d0*pi
C Take RM=50 cm reference radius, as this (arbitray) value is found in other exercises
      RM = 50.d0
C dR is the radial distance between two nodes, good starting point is dR = 0.5 cm
      dR = 0.5d0              ! cm, mesh step in radius, approximate: allows getting NR
C dX=RM*dA is the arc length between two nodes along R=RM arc, given angle increment dA
C A good starting point (by experience) is dX a few mm, say ~0.5 cm
      dX = 0.5d0              ! cm, mesh step at RM, approximate: allows getting NX

C------------ Outcomes :
C Radial extent of the field map
      Rmi = 1.d0   ! cm
      Rma = 76.d0   ! cm
      NR = NINT((Rma - Rmi) / dR) +1
      dR = (Rma - Rmi) / dble(NR -1)   ! make sure (NR-1)*dR == Rma-Rmi
C dX=RM*dA is the arc length between two nodes along R=RM arc, given angle increment dA
      NX = NINT(RM*AT / dX)  +1
      dX = RM*AT / DBLE(NX - 1)  ! exact mesh step at RM, corresponding to NX
      dA = dX / RM              ! corresponding delta_angle
      A1 = 0.d0 ; A2 = AT
C------------------------------------------
      BY = 0.d0 ; BX = 0.d0 ; Z = 0.d0
      BZ = 5.d0 ! kG

      open(unit=2,file='geneSectorMap.out')
      write(2,*) Rmi,dR,dA/pi*180.d0,dZ,
     >'     ! Rmi/cm, dR/cm, dA/deg, dZ/cm'
      write(2,*) '# Field map generated using geneSectorMap.f '
      write(2,fmt='(a)') '# AT/rd,  AT/deg, Rmi/cm, Rma/cm, RM/cm,'
     >//' NR, dR/cm, NX, dX/cm, dA/rd : '
      write(2,fmt='(a,1p,5(e16.8,1x),2(i3,1x,e16.8,1x),e16.8)')
     >'# ',AT, AT/pi*180.d0,Rmi, Rma, RM, NR, dX, NX, dX, dA
      write(2,*) '# For TOSCA: ',NX,NR,' 1 22.1 1.  !IZ=1 -> 2D ; '
     >//'MOD=22 -> polar map ; .MOD2=.1 -> one map file'
      write(2,*) '# R*cosA (A:0->360), Z==0, R*sinA, BY, BZ, BX '
      write(2,*) '# cm              cm     cm      kG  kG  kG '
      write(2,*) '# '

      do jr = 1, NR
        R = Rmi + dble(jr-1)*dR
        do ix = 1, NX
          A = A1 + dble(ix-1)*dA
C         write(2,fmt='(1p,6(e16.8),a)')  R, Z, A, BR, BZ, BA
          X = R * sin(A)
          Y = R * cos(A)
          write(2,fmt='(1p,6(e16.8),2(1x,i0))')  Y,Z,X,BY,BZ,BX,ix,jr
        enddo
      enddo

      stop ' Job complete ! Field map stored in geneSectorMap.out.'
      end
```

Zgoubi optical sequence using `TOSCA`

A uniform field 180 degree sector dipole field map in cylindrical coordinates,

1.5. Appendix   19

```
! used twice so to simulate a 360 degree cyclotron dipole.
! A 200 keV proton is tracked through. Its step-by-step coordinates are logged to zgoubi.plt.
 'OBJET'
64.62444403717985                                        ! Rigidity (kG.cm), 200keV proton.
2
1 1
12.9248888074 0. 0. 0. 0. 1. 'm'            ! Injection radius (all other coordinates zero).
1

 'PARTICUL'              ! This is required only because we want to get the time-of-flight,
938.27208 1.602176487D-19 1.79284735 0. 0.    ! raytracing otherwise just requires rigidity.
! PROTON                                        ! An alternate way to define a proton.

 'FAISTORE'
zgoubi.fai   #End     ! #End tells where (at which subsequent labeled keyword), particle
1                     ! data are to be logged to zgoubi.fai.
 'TOSCA'              ! First 180 degree field map
0  2                 ! IL=2 here logs the step-by-step proton coordinates to zgoubi.plt.
1.  1.  1.  1.
HEADER_8
315 121 1 22.1 1.    ! IZ=1 -> 2D ; MOD=22 -> polar map ; .MOD2=.1 -> single map.
geneSectorMap.out
0 0 0
2                    ! 9*9 node grid for second order fiel interpolation.
1.                   ! 1 cm step size.
2
0. 0. 0. 0.
 'TOSCA'             ! Second 180 degree field map
0  2                 ! IL=2 here logs the step-by-step proton coordinates to zgoubi.plt.
1.  1.  1.  1.
HEADER_8
315 121 1 22.1 1.    ! IZ=1 -> 2D ; MOD=22 -> polar map ; .MOD2=.1 -> single map
geneSectorMap.out
0 0 0 0
2                    ! 9*9 node grid for second order fiel interpolation
1.                   ! 1 cm step size
2
0. 0. 0. 0.

 'FAISCEAU'  #End      ! Label '#End' tells 'FAISTORE' to log particle data here!
 'END'
```

1.5.2   *Optical sequence using* `DIPOLE`

The cyclotron is defined using a mathematical model for the dipole field, a 60° sector, here. This optical sequence can be copy-pasted to a Zgoubi input data file and run as it is.

```
Cyclotron, classical.
 'OBJET'
64.62444403717985                           ! 200keV
2
4 1
12.9248888074 0.  0.   0.   0.  1. 'm'        ! 200keV. R=Brho/B=*/.5
28.9070891209 0.  0.   0.   0.  2.23654451125 'm'  ! 1 MeV. R=Brho/B=*/.5
50.          0.  0.   0.   0.  3.86850523397 'o'  ! at RM  (B*rho=0.5*0.5=0.25T.m, 2.9885 MeV)
64.7070336799 0. 0.   0.   0.  5.0063899693 'M'   ! 5 MeV. R=Brho/B=*/.5
1 1 1 1

 'DIPOLE'
0
60. 50.
30.  5. 0. 0. 0.
0.  0.                                      ! EFB 1  hard-edge
4  .1455   2.2670  -.6395  1.1558  0. 0.  0.
30. 0.  1.E6  -1.E6  1.E6  1.E6
0.  0.                                      ! EFB 2
4  .1455   2.2670  -.6395  1.1558  0. 0.  0.
-30. 0.  1.E6  -1.E6  1.E6  1.E6
0. 0.                                       ! EFB 3
0  0.      0.     0.      0.      0. 0. 0.
0. 0.  1.E6  -1.E6  1.E6  1.E6 0.
4   10.
1.                   ! The smaller, the better the orbits close.
2  0. 0. 0. 0.       ! Could also be, e.g., 2 50. 0. 50. 0. with Y0 amended accordingly in OBJET
 'FAISCEAU'
 'FAISTORE'
zgoubi.fai
1
 'END'
```

20 *Cyclotron*

Bibliography

[1] E.O.Lawrence and N.E.Edlefsen, Science 72, 376 (1930);
E.O.Lawrence and M.S. Livingston, Phys. Rev. 37 (1931), 1707; 38, 136, (1931); 40, 19 (1932)

[2] T. Kawaguchi et al., Design of the sector magnets for the RIKEN superconducting ring cyclotron, Proceedings of the 15th International Conference on Cyclotrons and their Applications, Caen, France.
http://www.nishina.riken.jp/facility/SRC_e.html

[3] H.A.Bethe and M.E.Rose, Phys. Rev. 54, 588 (1938)

[4] 4.a L.H.Thomas, *The Paths of Ions in the Cyclotron*, Phys. Rev. 54, 580, (1938)
4.b M.K. Craddock, *AG focusing in the Thomas cyclotron of 1938* , Proceedings of PAC09, Vancouver, BC, Canada, FR5REP1.

[5] F. Chautard, *Beam Dynamics For Cyclotrons*, in *CERN Accelerator School*, Zeegse, The Netherlands, 24 May-2 June 2005.

[6] J. Le Duff, *Longitudinal beam dynamics in circular accelerators*, in *CERN Accelerator School*, Jyvaskyla, Finland, 7-18 September 1992.

[7] T. Stammbach, *Introduction to Cyclotrons*, in *CERN accelerator school, cyclotrons, linacs and their applications*, IBM International Education Centre, La Hulpe, Belgium, 28 April-5 May 1994.

[8] H. A. Enge, Deflecting magnets, in Focusing of Charged Particles, Vol. 1, A. Septier Ed., Academic Press (1967).

[9] G. Leleux, Circular accelerators, INSTN lectures, SATURNE Laboratory, CEA Saclay (Juin 1978). Some passages of the present document are inspired from these lectures.